

Enhanced intersubband absorption due to impurity particles inside the insulator region of a metal-insulator-semiconductor system

Ten-Ming Wu* and Shou-yih Wang

Physics Department, National Tsing Hua University Hsinchu, Taiwan 300, Republic of China

(Received 5 February 1985; revised manuscript received 11 September 1985)

The only existing theory, developed by Nee, for the enhanced intersubband infrared absorption in a metal-insulator-semiconductor system due to dielectric irregularities has been significantly extended. We have rederived the relevant absorption formulas with reduction of some of the approximations used in Nee's paper and obtained more-general results. With these more-transparent formulas we can qualitatively explain some experimental data. Correlations between the experimental and theoretical power absorption are analyzed and discussed. A model is proposed. The calculated absorption spectra of this model are generally broadened and enhanced when including more possible transition momenta.

I. INTRODUCTION

There are many studies, both experimental and theoretical, of the intersubband resonance in a metal-insulator-semiconductor (MIS) system. It has been observed in Si,¹ Ge,² InAs,³ and InSb,^{4,5} using far-infrared subband resonance spectroscopy. The major resonance peaks of the absorption spectra are interpreted in the literature as collective modes with the macroscopic depolarization fields.⁶ In contrast to the spectrum of Si, it has been observed that a doublet structure appears together with the major resonance peaks in the spectra of Ge, InAs, and InSb. The doublet has been tentatively proposed to be produced by the nonparabolicity of the subbands. However, this explanation fails to explain the doublet² in Ge(111), where only a parabolic subband is involved.

Wiesinger, Reisinger, and Koch⁵ suggests that the doublet structure for the 0→1 transition in the case of InSb represents two different excitation modes of the surface electrons. They postulated the existence of a small Rayleigh-scattering perpendicular component of the internal field due to dielectric irregularities in the lacquer coating layer at the semiconductor-insulator interface.

The fundamental theory of absorption due to dielectric irregularities was given by Nee.⁶ In his treatment a parabolic-band-structure approximation for surface electrons in an inversion or accumulation layer is used. The numerical aspects of this work have been subsequently given by Nee and Koch.⁷ In the following we will recapitulate Ref. 6 because what we report here is in some sense an extension of that work. The motion of the surface electrons can be described by the wave function⁸

$$\psi_{l\mathbf{k}} = \frac{1}{A^{1/2}} e^{i\mathbf{k}\cdot\mathbf{r}} \psi_l(z)$$

with subband energy

$$\epsilon_{l\mathbf{k}} = \frac{\hbar^2 k^2}{2m_t} + \epsilon_l,$$

where ϵ_l and ψ_l ($l=0,1,2,\dots$) are, respectively, the ener-

gy and wave function associated with the quantized motion in the direction normal to the semiconductor-insulator interface. The area of the interface is A . m_t and m_l are, respectively, the electronic effective mass parallel and perpendicular to the interface. \mathbf{r} and $\hbar\mathbf{k}$ denote the coordinate vector and momentum vector in the two-dimensional interface plane, respectively.

The effective potential $V_{\text{eff}}(z)$ which the surface charge carriers "feel" in the direction of the applied external electrical field consists of the usual electrostatic potential including the Hartree potential of the electrons themselves and the exchange-correlation potential. Both the effective potential including the correlation effect and the energy splitting between the ground and the excited subband for the Si(100) case have been calculated by Ando.^{9,10} The calculated energy splitting for the accumulation case agrees with the experimental value. But for the inversion case, the calculated energies are larger than the experimental data.

In this paper, we assume that the interface is sharp and that there is an infinite barrier which keeps electrons out of the insulator. For mathematical convenience, we approximate the effective potential by a triangular well,¹¹ that is

$$V(z) = \begin{cases} eFz & \text{for } z > 0, \\ +\infty & \text{for } z < 0, \end{cases}$$

$$F = \frac{4\pi(N_{\text{depl}} + fN_s)e}{\epsilon_s},$$

where N_{depl} is the concentration of fixed space charges in the depletion layer and N_s is the density of electrons per unit area in an inversion or accumulation layer. We let f be a parameter such that the energy splittings of the triangular potential are the same as those of Ando's values.⁹ For the Si(100) n -inversion case, the potential is shown in Fig. 1.

The Schrödinger equation in the z direction is exactly solved with the condition that the envelope wave functions goes to zero at $z=0$ and at infinity. The eigenfunc-

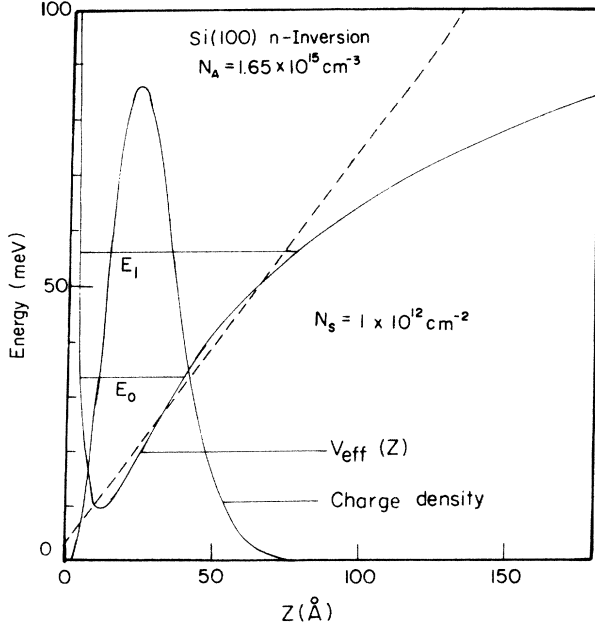


FIG. 1. Effective potential $V_{\text{eff}}(z)$ and surface charge density for a Si(100) n -inversion layer calculated by Ando (Ref. 9). The dashed curve is the approximate triangle potential we used in this paper, $eF=0.708$ meV/Å, $a_0=(\hbar^2/2m_l eF)^{1/3}=18.05$ Å, $\omega_{10}=\epsilon_1-\epsilon_0/\hbar=\hbar k_0^2/2m_l=3.40\times 10^{13}$ s $^{-1}$, $k_0=1.06\times 10^8$ cm $^{-1}$, $N_{\text{depl}}=1.55\times 10^{-11}$ cm $^{-2}$.

tions $\psi_l(z)$ are Airy functions $\phi_l(z)$:¹²

$$\psi_l(z)=A_l\phi\left[\frac{z}{a_0}-\alpha_l\right], \quad (1.1)$$

where A_l are normalizing factors, $-\alpha_l$ are the roots of the Airy function ($l=0,1,2,\dots$), $a_0=(\hbar^2/2m_l eF)^{1/3}$ and $\epsilon_l=\alpha_l[(eF\hbar)^2/2m_l]^{1/3}$.

In Sec. II the absorption coefficients associated with any surface electron transition momentum $\hbar\mathbf{q}$ parallel to the interface are derived assuming $q \gg (\epsilon_s)^{1/2}\omega/c$. ω and ϵ_s are the frequency of incident light, and the dielectric constant of the semiconductor, respectively. In Sec. III we summarize the absorption coefficient formulas for the three cases derived in Sec. II into a general form. One model of the distribution of the dielectric irregularities is proposed in Sec. IV. The spectrum lines are generally broadened when including more possible transition momenta. These results are also given.

II. ABSORPTION COEFFICIENTS

From the semiconductor region of a MIS system, a monochromatic electromagnetic wave of angular frequency ω is incident on the semiconductor-insulator interface with an angle of incidence θ . It will be partly reflected by the interface and partly transmitted into the insulator region of the dielectric constant ϵ_i . If there are impurity particles near the interface within the insulator, the transmitted wave can be scattered by these particles. The scattered electromagnetic field should interact with the

surface electrons inside the accumulation or inversion layer of the semiconductor and this enhances the absorption. Figures 2(a) and 2(b) are cited from Ref. 6 in order to show conveniently how these waves intercorrelate.

From the definition of the spectral function $\underline{Z}_{l'l}(\mathbf{q})$ given in Ref. 6, the impurity-induced power absorption per unit area by the surface-charge carriers can be readily written as

$$P_s^{(b)} = \sum_{\mathbf{q}} \hbar\omega e^2 \text{Re} \left[-i \sum_{l',l} \underline{E}_{l'l}(\mathbf{q}) \cdot \underline{Z}_{l'l}(\mathbf{q}) \cdot \underline{E}_{l'l}(\mathbf{q}) \right], \quad (2.1)$$

where $\hbar\mathbf{q}$ is the two-dimensional transition momentum parallel to the interface. The electric field matrix elements for $l' \rightarrow l$ intersubband transition $\underline{E}_{l'l}(\mathbf{q})$ are expressed⁶ as

$$\underline{E}_{l'l}(\mathbf{q}) = [\underline{E}_0(\mathbf{q})]_{l'l} + [\underline{\Delta E}(\mathbf{q})]_{l'l}, \quad (2.2)$$

where the definitions of $[\underline{E}_0(\mathbf{q})]_{l'l}$ and $[\underline{\Delta E}(\mathbf{q})]_{l'l}$ are the same as those in Ref. 6. $[\underline{\Delta E}(\mathbf{q})]_{l'l}$ are the depolarization field contributions due to surface-charge carriers inside the accumulation or inversion layers. As in the approximation I in Ref. 6, we neglect the coupling between the $l \rightarrow l'$ intersubband transition and the $m \rightarrow m'$, $mm' \neq ll'$,

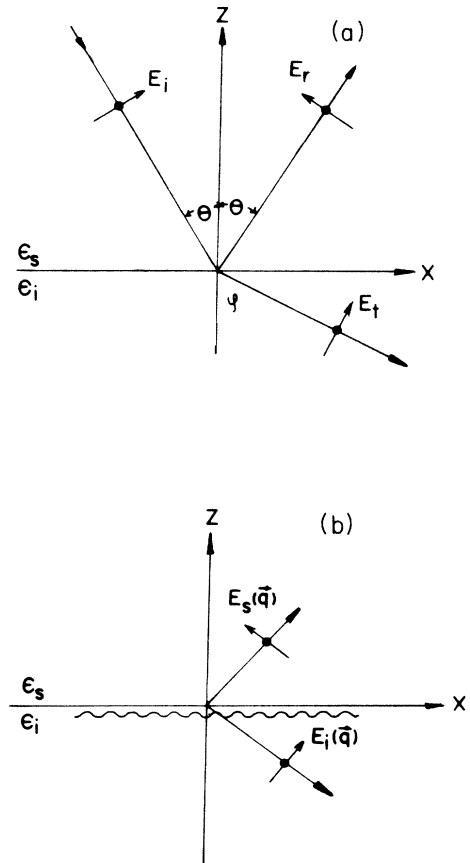


FIG. 2. (a) Incident, reflected and transmitted waves at the IS interface. (b) Electromagnetic waves scattered by the surface irregularities (cited from Ref. 6).

and obtain

$$[\underline{\Delta E}(\mathbf{q})]_{l'l} \simeq -\underline{\chi}'_{l'l}(\mathbf{q}) \cdot \underline{E}_{l'l}(\mathbf{q}). \quad (2.3)$$

For any \mathbf{q} , expressed in polar coordinates (q, ϕ) , i.e.,

$\mathbf{q} = (q \cos \phi, q \sin \phi, 0)$, $\underline{\chi}'_{l'l}(\mathbf{q})$ can be rearranged as

$$\underline{\chi}'_{l'l}(\mathbf{q}) = \frac{8\pi\hbar e^2}{\epsilon_s} \tilde{u}_{l'l} [\underline{R}_s(q, \phi)]_{l'l} \underline{Z}_{l'l}(q, \phi). \quad (2.4)$$

where $\tilde{u}_{l'l}$ are the same as in Ref. 6 and

$$[\underline{R}_s(q, \phi)]_{l'l} = \begin{pmatrix} (q^2 \cos^2 \phi - q_0^2) \frac{\hbar^2}{m_l^2 \omega_{l'l}^2} & q^2 \cos \phi \sin \phi \frac{\hbar^2}{m_l^2 \omega_{l'l}^2} & -iq \cos \phi \frac{\hbar}{m_l \omega_{l'l}} \\ q^2 \cos \phi \sin \phi \frac{\hbar^2}{m_l^2 \omega_{l'l}^2} & (q^2 \sin^2 \phi - q_0^2) \frac{\hbar^2}{m_l^2 \omega_{l'l}^2} & -iq \sin \phi \frac{\hbar}{m_l \omega_{l'l}} \\ iq \cos \phi \frac{\hbar}{m_l \omega_{l'l}} & iq \sin \phi \frac{\hbar}{m_l \omega_{l'l}} & 1 \end{pmatrix}, \quad (2.5)$$

with

$$q_0^2 = \epsilon_s \frac{\omega^2}{c^2},$$

$$\omega_{l'l} = \frac{\epsilon_l - \epsilon_l}{\hbar}.$$

Since the elements of $[\underline{R}_s(q, \phi)]_{l'l}$ have different dimensions, there is no good reason to omit the terms of xz and yz elements in (2.5). We think the approximation II of Ref. 6 of omitting these couplings is not quite satisfactory. Therefore, we keep these terms in this paper and obtain some different results.

Substituting (2.3), (2.4) into (2.2), we obtain

$$[\underline{E}_0(\mathbf{q})]_{l'l} = [\underline{\epsilon}(\mathbf{q})]_{l'l} \cdot \underline{E}_{l'l}(\mathbf{q})$$

and

$$[\underline{\epsilon}(\mathbf{q})]_{l'l} = \underline{I}_3 + \left[\frac{1}{A} \right] \cdot \underline{\chi}'_{l'l}(\mathbf{q}) \cdot [A],$$

where

$$[A] = \begin{pmatrix} 1 & 0 & 0 \\ 0 & 1 & 0 \\ 0 & 0 & A \end{pmatrix}, \quad \left[\frac{1}{A} \right] = \begin{pmatrix} 1 & 0 & 0 \\ 0 & 1 & 0 \\ 0 & 0 & \frac{1}{A} \end{pmatrix},$$

in which $A = (2m_l \hbar / m_l^2 \omega_{l'l})^{1/2}$ and its dimension is $[L]$. $\underline{\chi}'_{l'l}(\mathbf{q})$ is called the "effective susceptibility tensor" for the ll' -intersubband transition and is dimensionless.

As in approximation III of Ref. 6, we assume $q \gg (\epsilon_s)^{1/2} \omega / c$. $\underline{\chi}'_{l'l}(\mathbf{q})$ then becomes very simple in its mathematic expression:

$$\underline{\chi}'_{l'l}(\mathbf{q}) = \chi_0 \begin{pmatrix} \tilde{c}X \cos^2 \phi & \tilde{c}Y \cos \phi \sin \phi & -i\tilde{c}^{1/2} \tilde{\zeta}_{l'l} \cos \phi \\ \tilde{c}X \cos \phi \sin \phi & \tilde{c}Y \sin^2 \phi & -i\tilde{c}^{1/2} \tilde{\zeta}_{l'l} \sin \phi \\ i\tilde{c}^{1/2} X \cos \phi & i\tilde{c}^{1/2} Y \sin \phi & \tilde{\zeta}_{l'l} \end{pmatrix}, \quad (2.6)$$

where

$$\chi_0 = \frac{2e^2 m_l}{\epsilon_s m_l^2 \omega_{l'l}^2} \tilde{u}_{l'l}, \quad \tilde{c} = \frac{\hbar q^2}{2m_l \omega_{l'l}},$$

$$X = \frac{16\pi\hbar^2 \omega_{l'l}}{m_l^2} \left[\xi_{l'l}^{(1)} (\cos^2 \phi - \sin^2 \phi) + \xi_{l'l} \sin^2 \phi + \eta_{l'l} \cos^2 \phi + \frac{q^2}{8} \zeta_{l'l} \right],$$

$$Y = \frac{16\pi\hbar^2 \omega_{l'l}}{m_l^2} \left[\xi_{l'l}^{(1)} (\sin^2 \phi - \cos^2 \phi) + \xi_{l'l} \cos^2 \phi + \eta_{l'l} \sin^2 \phi + \frac{q^2}{8} \zeta_{l'l} \right],$$

$$\tilde{\zeta}_{l'l} = \frac{4\pi\hbar \omega_{l'l}^2}{m_l} \zeta_{l'l}.$$

The definitions of $\xi_{l'l}$, $\eta_{l'l}$, and $\zeta_{l'l}$ are the same as those in Ref. 6, and we have

$$\xi_{rl}^{(1)} = \frac{1}{2A} \sum_{\mathbf{k}} \frac{\eta_{l\mathbf{k}} - \eta_{l\mathbf{k}+\mathbf{q}}}{\omega_{l\mathbf{k}+\mathbf{q},l\mathbf{k}}^2 [\omega_{l\mathbf{k}+\mathbf{q},l\mathbf{k}}^2 - (\omega + ir)^2]} (k^2 \cos^2 \theta'),$$

where θ' is the angle between \mathbf{k} and \mathbf{q} .

As can be seen from Eq. (2.6), the elements of $\underline{\chi}_{rl}(\mathbf{q})$

$$\underline{\epsilon}_{rl}^{-1}(\mathbf{q}) = \left[\frac{1}{A} \right] \cdot \tilde{\underline{\epsilon}}_{rl}^{-1}(\mathbf{q}) \cdot [A],$$

$$\tilde{\underline{\epsilon}}_{rl}^{-1}(\mathbf{q}) = \frac{1}{|\det \tilde{\underline{\epsilon}}_{rl}|} \begin{pmatrix} 1+x_{22}+x_{33} & -x_{12} & -x_{13} \\ -x_{21} & 1+x_{11}+x_{33} & -x_{23} \\ -x_{31} & -x_{32} & 1+x_{11}+x_{22} \end{pmatrix}_{rl},$$

where

$$|\det \tilde{\underline{\epsilon}}_{rl}| = |1+x_{11}+x_{22}+x_{33}|_{rl} = |1+\text{Tr} \underline{\chi}_{rl}(\mathbf{q})|$$

and consequently,

$$\underline{E}_{rl}(\mathbf{q}) = \underline{\epsilon}_{rl}^{-1}(\mathbf{q}) \cdot [\underline{E}_0(\mathbf{q})]_{rl}. \quad (2.7)$$

From Ref. 6,

$$[\underline{E}_0(\mathbf{q})]_{rl} = f_{rl} \cdot \underline{E}_s(\mathbf{q}). \quad (2.8)$$

Assuming that each impurity particle has electric polarizability α_i and the distribution in the insulator region is $n(x)$, $\underline{E}_s(\mathbf{q})$ is related to $n(\mathbf{q}, z)$, the two-dimensional Fourier transform of $n(x)$ via the polarization transfer operator matrix, $\underline{t}_s(\mathbf{q})$,

$$\underline{E}_s(\mathbf{q}) = N(\mathbf{q}) \underline{t}_s(\mathbf{q}) \cdot \underline{E}_t, \quad (2.9)$$

where

$$N(\mathbf{q}) = \alpha_i \int_{-\infty}^0 dz n(\mathbf{q}, z) e^{-i(q_i + q_{1i})z}. \quad (2.10)$$

The expression of $\underline{t}_s(\mathbf{q})$ has been given explicitly in Ref. 6. It is a characteristic tensor of the surface scattering mechanism and contains no information about the distribution of impurity particles. In the assumption, $q \gg (\epsilon_s)^{1/2} \omega / c$,

$$q_{1i} = \left[\epsilon_i \frac{\omega^2}{c^2} - q^2 \right]^{1/2} \simeq iq \left[1 - \frac{\epsilon_i \omega^2}{2c^2 q^2} \right].$$

$\underline{t}_s(\mathbf{q})$ can be simplified as

$$\underline{t}_s(\mathbf{q}) \simeq - \frac{4\pi q}{(\epsilon_s + \epsilon_i)} \times \begin{pmatrix} \cos^2 \phi & \cos \phi \sin \phi & i \cos \phi \\ \cos \phi \sin \phi & \sin^2 \phi & i \sin \phi \\ i \cos \phi & i \sin \phi & -1 \end{pmatrix}.$$

\underline{E}_t is the amplitude of the transmitted electric field, and is related to that of the incident electric field \underline{E}_{i0} via proper boundary conditions. The relation is

$$\underline{E}_t = \underline{\Phi}_t \cdot \underline{E}_{i0}, \quad (2.11)$$

obey the following relations:

- (i) $\det[\underline{\chi}_{rl}(\mathbf{q})] = 0$,
- (ii) the determinant of any minor of $\underline{\chi}_{rl}(\mathbf{q})$ is also zero.

Using these relations we invert the effective dielectric tensor $\underline{\epsilon}_{rl}(\mathbf{q})$:

where

$$\underline{\Phi}_t = \begin{pmatrix} \alpha_{||} \cos \psi & 0 \\ 0 & \alpha_{\perp} \\ \alpha_{||} \sin \psi & 0 \end{pmatrix},$$

$$\alpha_{||} = \frac{2(\epsilon_s)^{1/2} \cos \theta}{(\epsilon_i)^{1/2} \cos \theta + (\epsilon_s)^{1/2} \cos \psi},$$

$$\alpha_{\perp} = \frac{2(\epsilon_s)^{1/2} \cos \theta}{(\epsilon_i)^{1/2} \cos \psi + (\epsilon_s)^{1/2} \cos \theta}.$$

Substitution of Eqs. (2.7) and (2.8) into Eq. (2.1) yields the enhanced power absorption per unit area of surface charge carriers in the semiconductor region:

$$P_s^{(b)} = \sum_{\mathbf{q}} \text{Re}[-i \underline{E}_s^{\dagger}(\mathbf{q}) \cdot \underline{V}(\mathbf{q}) \cdot \underline{E}_s(\mathbf{q})], \quad (2.12)$$

where

$$\underline{V}(\mathbf{q}) = \hbar \omega e^2 \sum_{r,l} (f_{rl})^{\dagger} \cdot [\underline{\epsilon}_{rl}^{-1}(\mathbf{q})]^{\dagger} \cdot \underline{Z}_{rl}(\mathbf{q}) \cdot \underline{\epsilon}_{rl}^{-1}(\mathbf{q}) \cdot f_{rl}.$$

Substituting Eqs. (2.9), (2.11) into Eq. (2.12) the power absorption per area becomes

$$P_s^{(b)} \simeq \sum_{\mathbf{q}} \text{Re}[-i |N(\mathbf{q})|^2 \underline{E}_{i0}^{\dagger} \cdot \underline{A}(\mathbf{q}, \omega, \theta) \cdot \underline{E}_{i0}].$$

The derivation of $\underline{A}(\mathbf{q}, \omega, \theta)$ is lengthy and will be reported elsewhere. The results are given below.

For the case $\theta > \sin^{-1}(\epsilon_i / \epsilon_s)^{1/2}$, which is the critical angle θ_c ,

$$\underline{E}_{i0} = \begin{pmatrix} E_{i||} \\ E_{i\perp} \end{pmatrix}$$

and $\underline{A}(\mathbf{q}, \omega, \theta)$ takes the form

$$\underline{A}(\mathbf{q}, \omega, \theta) \simeq \frac{2\pi \epsilon_s}{(\epsilon_i + \epsilon_s)^2} \frac{m_l^2 \omega}{\hbar^2} \times \sum_{r,l} \frac{\omega_{rl}^2 |f_{rl}(\mathbf{q})|^2}{\tilde{u}_{rl}} \frac{\chi_{rl}}{|1 + \chi_{rl}|^2} \begin{pmatrix} A_{11} & A_{12} \\ A_{21} & A_{22} \end{pmatrix},$$

where

$$f_{rl}(\mathbf{q}) = \int_0^\infty dz \psi_r(z) \psi_l(z) e^{iq_1 z},$$

$$\chi_{rl} = \text{Tr} \underline{\chi}_{rl}(\mathbf{q}) = (\chi_{11} + \chi_{22} + \chi_{33})_{rl} \\ = \chi_0 [\tilde{c}(X \cos^2 \phi + Y \sin^2 \phi) + \tilde{\zeta}_{rl}],$$

$$A_{11} = |\alpha_{ll}|^2 \left| \cos \phi \left[\frac{\epsilon_s}{\epsilon_i} \sin^2 \theta - 1 \right]^{1/2} - \left[\frac{\epsilon_s}{\epsilon_i} \right]^{1/2} \sin \theta \right|^2,$$

$$A_{12} = A_{21}^* = i \alpha_{ll}^* \alpha_{11} \sin \phi \\ \times \left[\cos \phi \left[\frac{\epsilon_s}{\epsilon_i} \sin^2 \theta - 1 \right]^{1/2} - \left[\frac{\epsilon_s}{\epsilon_i} \right]^{1/2} \sin \theta \right],$$

$$A_p^{(b)} = a_p^{(i)} \sum_{\mathbf{q}} |N(\mathbf{q})|^2 S(\mathbf{q}, \omega) \left| \cos \phi \left[\frac{\epsilon_s}{\epsilon_i} \sin^2 \theta - 1 \right]^{1/2} - \left[\frac{\epsilon_s}{\epsilon_i} \right]^{1/2} \sin \theta \right|^2, \quad (2.13)$$

$$A_s^{(b)} = a_s^{(i)} \sum_{\mathbf{q}} |N(\mathbf{q})|^2 S(\mathbf{q}, \omega) \sin^2 \phi, \quad (2.14)$$

where

$$S(\mathbf{q}, \omega) \simeq \frac{16\pi^2 \epsilon_s^{1/2} m_l^2 \omega}{(\epsilon_s + \epsilon_i)^2 \hbar^2 c} \sum_{r,l} \frac{\omega_{rl}^2 |f_{rl}(\mathbf{q})|^2}{\tilde{u}_{rl}} \frac{I_m \chi_{rl}}{|1 + \chi_{rl}|^2}, \quad (2.15)$$

$$a_p^{(i)} = \frac{4\epsilon_s \epsilon_i \cos \theta}{(\epsilon_i^2 \cos^2 \theta + \epsilon_s^2 \sin^2 \theta - \epsilon_i \epsilon_s)},$$

$$a_s^{(i)} = \frac{\epsilon_s \cos \theta}{\epsilon_s - \epsilon_i}.$$

For the normal-incidence case $\theta=0$,

$$\underline{E}_{i0} = \begin{bmatrix} E_{i0x} \\ E_{i0y} \\ 0 \end{bmatrix}.$$

E_{i0x} and E_{i0y} are the x component and y component, respectively, of the amplitude of the incident electric field:

$$\underline{A}(\mathbf{q}, \omega, \theta=0) \simeq \frac{2\pi \epsilon_s}{(\epsilon_s + \epsilon_i)^2} \frac{m_l^2 \omega}{\hbar^2} \\ \times \sum_{r,l} \frac{\omega_{rl}^2 |f_{rl}(\mathbf{q})|^2}{\tilde{u}_{rl}} \frac{\chi_{rl}}{|1 + \chi_{rl}|^2} \\ \times \begin{bmatrix} |\alpha|^2 \cos \phi & 0 & 0 \\ 0 & |\alpha|^2 \sin^2 \phi & 0 \\ 0 & 0 & 0 \end{bmatrix},$$

where

$$\alpha = \frac{2(\epsilon_s)^{1/2}}{(\epsilon_i)^{1/2} + (\epsilon_s)^{1/2}}.$$

The absorption coefficient for normal incidence is

$$A_n^{(b)} = a_n^{(i)} \sum_{\mathbf{q}} |N(\mathbf{q})|^2 S(\mathbf{q}, \omega) \\ \times \left[\frac{|E_{i0x}|^2 \cos^2 \phi + |E_{i0y}|^2 \sin^2 \phi}{|E_{i0x}|^2 + |E_{i0y}|^2} \right], \quad (2.16)$$

$$A_{22} = |\alpha_1|^2 \sin^2 \phi.$$

The enhanced absorption coefficient associated with impurity particles is defined as

$$A^{(b)} = P_s^{(b)} / P_0,$$

where P_0 is the total incident power per unit area,

$$P_0 = \frac{c^2}{8\pi\omega^2} q_s \underline{E}_{i0}^\dagger \cdot \underline{E}_{i0}.$$

For incident p -polarized and s -polarized waves, the absorption coefficients $A_p^{(b)}$ and $A_s^{(b)}$ are, respectively,

where

$$a_n^{(i)} = \frac{4\epsilon_s}{[(\epsilon_i)^{1/2} + (\epsilon_s)^{1/2}]^2}.$$

III. REARRANGING AND SUMMARIZING

From the three cases discussed above, we can rearrange the factors of $A_p^{(b)}$ and $A_s^{(b)}$ and summarize so that the expressions for the enhanced absorption coefficients due to impurity particles inside the insulator region are more transparent physically and take the general form of three major factors as in the following:

$$A^{(b)} = \sum_{\mathbf{q}} |N(\mathbf{q})|^2 S(\mathbf{q}, \omega) F(\theta, \phi). \quad (3.1)$$

(i) $S(\mathbf{q}, \omega)$ as given in Eq. (2.15) is the absorption spectrum function of intersubband transitions with the surface-charge-carrier momentum change $\hbar q$ parallel to the interface and the incident wave of angular frequency ω . It is related only to the two-dimensional intersubband system and has nothing to do with the distributions of impurity particles inside the insulator region. In general, for the 2π range of angle ϕ , $S(\mathbf{q}, \omega)$ is a periodic function of ϕ with period $\pi/2$. However, in the example of the Si(100) n -inversion layer, calculated by computer, it shows a very weak dependence on angle ϕ , even if we change the q and ω values. The q dependence of $S(\mathbf{q}, \omega)$ is shown in Fig. 3.

(ii) $F(\theta, \phi)$ is the polarization factor which characterizes mainly the polarization of the incident wave. It also depends upon the incident angle θ and the direction angle ϕ of the two-dimensional transition momentum q .

There are two sources of the polarization factor. One is the transmission coefficient $a^{(i)}$, arising from the back and forth transmission of the electromagnetic wave through the semiconductor-insulator interface. The other one is the impurity-particle scattering mechanism.

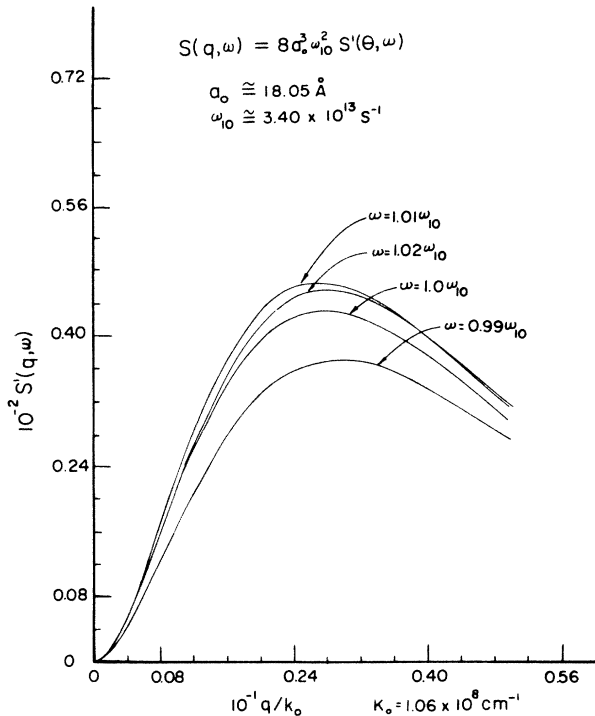


FIG. 3. Function $S'(q, \omega)$ vs q , $S(q, \omega) \cong 8a_0^3 \omega_0^2 S'(q, \omega)$.

For incident angle $\theta > \theta_c$, and p -polarized waves,

$$F(\theta, \phi) = a_p^{(i)} \left| \cos \phi \left[\frac{\epsilon_s}{\epsilon_i} \sin^2 \theta - 1 \right]^{1/2} - \left[\frac{\epsilon_s}{\epsilon_i} \right]^{1/2} \sin \theta \right|^2.$$

For s -polarized waves,

$$F(\theta, \phi) = a_s^{(i)} \sin^2 \phi.$$

At normal incidence $\theta = 0$,

$$F(\theta, \phi) = a_n^{(i)} \left[\frac{|E_{i0x}|^2 \cos^2 \phi + |E_{i0y}|^2 \sin^2 \phi}{|E_{i0x}|^2 + |E_{i0y}|^2} \right]. \quad (3.2)$$

Although $S(q, \omega)$ is very weakly dependent on ϕ , the polarization factor $F(\theta, \phi)$ is quite dependent on it. For $\theta = 45^\circ$, $F(\theta, \phi)$ for the Si-SiO₂ interface for p waves and s waves are shown, respectively, in Fig. 4. For any mode q with angle θ , this factor for p waves will be larger than that for s waves. Thus, no matter what the distribution of impurity particles inside the insulator region is, the absorption coefficient for p -polarized light is always larger than that for the s -polarized light. This is also true for the derivative of the absorption coefficient with respect to the surface-charge density N_s . This qualitatively agrees with the experimental results for InSb (Ref. 5) and InAs.³

It has been shown that gratings can be used to excite the intersubband resonance on Si(100) with normal-incidence light.¹³ It is excited by a normal component electric field, which is induced by the structure gate electrode. The comparison of the experimental results for $dA^{(b)}/dN_s$ with those calculated from Nee's theory has been given in Ref. 14. But, with the polarization factor, we can give some simple general arguments.

If the grating stripes are in the x direction according to

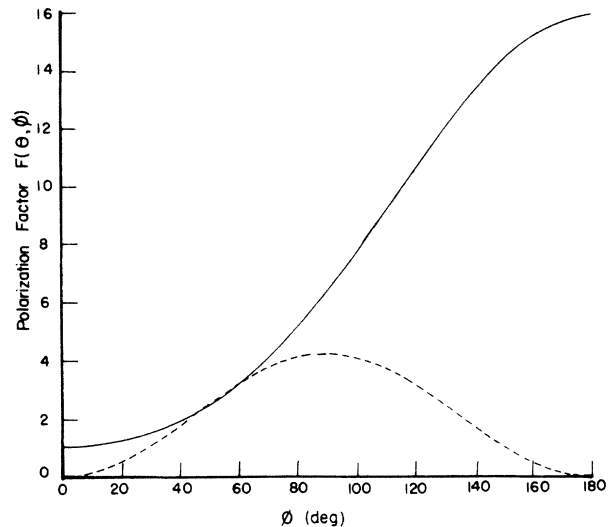


FIG. 4. Polarization factor function $F(\theta, \phi)$ versus angle ϕ for p waves (solid curve) and s waves (dashed curve) with incident angle $\theta = 45^\circ$.

Ref. 13, the modes excited by the gratings are $\mathbf{q} = (2n\pi/L, 0, 0)$ $n = 1, 2, 3, \dots$. Expressed in polar coordinates, $\mathbf{q} = (q = 2n\pi/L, \phi = 0)$. If the normal incident electric fields are perpendicular to the grating stripes, i.e.,

$$\underline{E}_{i0} = \begin{bmatrix} E_{i0x} \\ 0 \\ 0 \end{bmatrix},$$

according to Eq. (3.2), the polarization factor will be a constant, totally arising from the transmission coefficient. However, if the electric fields are parallel to the grating stripes, i.e.,

$$\underline{E}_{i0} = \begin{bmatrix} 0 \\ E_{i0y} \\ 0 \end{bmatrix},$$

then $F(\theta, \phi) = 0$ for all \mathbf{q} . Therefore, there will be no absorption at all. But the absorption formulas we obtain in this paper are of the first-order approximation only. So, we expect the absorption for the parallel-polarized incident light to be extremely small.

(iii) $|N(\mathbf{q})|^2$ may be regarded as the coupling coefficient of the enhanced absorption spectrum function $S(\mathbf{q}, \omega)$. It depends upon the distribution of impurity particles inside the insulator region. So, the absorption coefficients will be different for different distributions.

In the next section, we propose a distribution model for the impurity particles and will calculate the associated absorption coefficients. Before doing so, we must consider the relation between the absorption coefficients calculated from theory and those obtained from experiments.

From the viewpoint of experiments, the absorbance is defined as

$$P_{\text{expt}} = -[T(V_g) - T(V_t)]/T(V_t)$$

(Ref. 12), where $T(V_g)$ and $T(V_t)$ are the transmission through the MIS capacitor with gate voltage V_g and

threshold voltage V_t , respectively. The power absorption due to the surface-charge carriers is $-[T(V_g) - T(V_t)]$. This corresponds to the quantity which we can calculate from (2.13), (2.14), and (2.16). Here, we denote the power absorption from theory as P_{theor} . Thus, we have,

$$P_{\text{expt}} = \frac{1}{T(V_t)} P_{\text{theor}}. \quad (3.3)$$

In laser spectroscopic experiments, the optical-absorption derivative dP_{expt}/dV_g is measured. Differentiating Eq. (3.3) with respect to V_g , we get

$$\frac{dP_{\text{expt}}}{dV_g} = \frac{1}{T(V_t)} \frac{dP_{\text{theor}}}{dV_g}.$$

Therefore, the experimental value, dP_{expt}/dV_g , is larger than that calculated from theory, dP_{theor}/dV_g , by a factor $1/T(V_t)$. This factor will be different for different experimental arrangements. Thus, it is difficult to calculate the experimental absorption derivative from theory. It is even more difficult using this approach to calculate the absolute value of the absorptance to compare it directly with experimental results. Therefore, it is worthy of note that only the relative values of the absorption coefficients as calculated from Eqs. (2.13), (2.14), and (2.16) and the shape of absorption spectrum lines are significant in comparison with experiments.

IV: A MODEL FOR THE IMPURITY PARTICLE DISTRIBUTION AND ITS ABSORPTION COEFFICIENTS

In this section, we propose a distribution model for the impurity particles inside the insulator region. We assume that there is one layer of a two-dimensional simple lattice at $z = -d$ with a sphere basis of radius R at each lattice point. As shown in Fig. 5, a and b are the fundamental units of the simple lattice in the X and Y directions, respectively. The distribution at a plane $Z = \text{const}$ in the primitive cells is

$$n(\mathbf{x}) = \sum_{\mathbf{q}} n(\mathbf{q}, z) e^{i\mathbf{q} \cdot \mathbf{r}},$$

$$n(\mathbf{q}, z) = \frac{2\pi n_0}{ab} \frac{[R^2 - (z+d)^2]^{1/2} J_1(q[R^2 - (z+d)^2]^{1/2})}{q} \delta_{\mathbf{q}, \mathbf{G}}, \quad (4.1)$$

where $J_1(x)$ is the Bessel function of the first order and

$$\mathbf{G} = \left[\frac{2\pi n}{a}, \frac{2\pi m}{b} \right], \quad n, m \text{ integers}.$$

For $\theta > \theta_c$ and by the assumption $q \gg (\epsilon_s)^{1/2} \omega/c$, q_i and $q_{\perp i}$ are all pure imaginary quantities, and $|q_{\perp i}| \gg |q_i|$. Substituting Eq. (4.1) into Eq. (2.10), we get

$$N(\mathbf{q}) = 3\alpha_i \frac{N}{ab} \frac{e^{-q_d}}{qR} \delta_{\mathbf{q}, \mathbf{G}} \int_0^1 (1-z'^2)^{1/2} J_1(qR(1-z'^2)^{1/2}) \cosh(qRz') dz',$$

where $z' = z + d/R$ and $N = (4\pi R^3/3)n_0$ is the total number of impurity particles inside each sphere basis. In Fig. 6, $|N(\mathbf{q})|^2$ is plotted as a function of qR for each d with the y axis in logarithmic scale. Because $|N(\mathbf{q})|^2$ decays

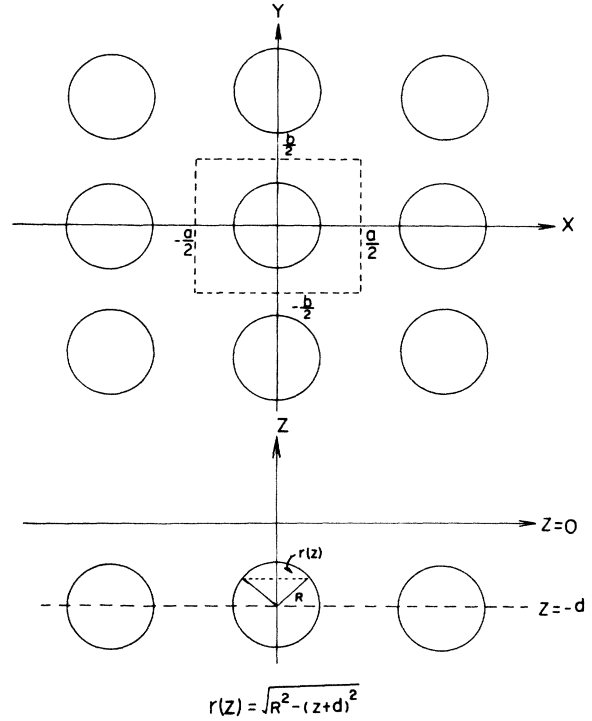


FIG. 5. Model of impurity-particle distribution with one layer of a two-dimensional simple lattice at $z = -d$ with a sphere basis of radius R at each lattice point.

$$n(\mathbf{x}') = \begin{cases} n_0 & \text{for } r' \leq r(z), \\ 0 & \text{otherwise,} \end{cases}$$

where $r(z) = [R^2 - (z+d)^2]^{1/2}$, with $|z+d| \leq R$. Because of the periodic structure, it is only the fundamental vector \mathbf{G} of the reciprocal lattice that will be in the Fourier transform of the impurity particles distribution. Therefore,

very fast with q , absorption with small- q values dominates the absorption coefficients.

In this model, we set $d = R = 360 \text{ \AA}$ and $a = b$ for a square lattice. The calculated absorption coefficients $A_p^{(i)}$

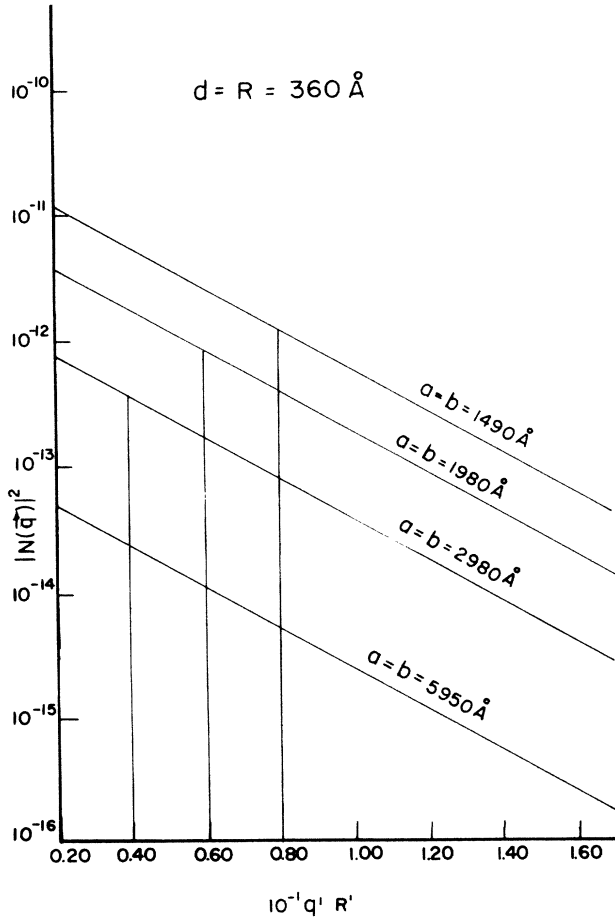


FIG. 6. Coupling coefficients $|N(\mathbf{q})|^2$ of the model used in this paper with $d=R=360 \text{ \AA}$. The abscissa is normalized with $q'=q/k_0$ and $R'=R_0/a_0$. The initial q values are also indicated.

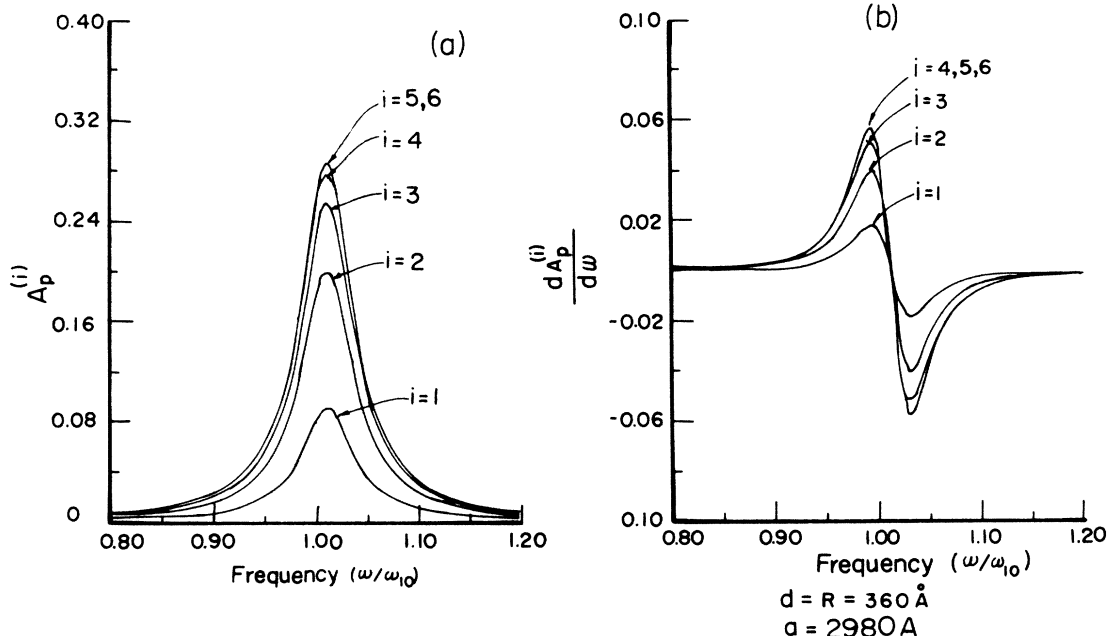


FIG. 7. (a) Calculated absorption spectra $A_p^{(i)}$ of the model for $R=360 \text{ \AA}$ and $a=2980 \text{ \AA}$. The abscissa is normalized with ω_{10} . With i up to 6, $i=1$ for 8 \mathbf{G} vectors, $i=2$ for 24 \mathbf{G} vectors, $i=3$ for 48 \mathbf{G} vectors, $i=4$ for 80 \mathbf{G} vectors, $i=5$ for 120 \mathbf{G} vectors, and $i=6$ for 168 \mathbf{G} vectors. (b) Calculated derivative absorption spectra $dA_p^{(i)}/d\omega$ of the model for $d=R=360 \text{ \AA}$ and $a=2980 \text{ \AA}$.

for $a=2980 \text{ \AA}$ are given in Fig. 7. In Fig. 7, there are N_i vectors \mathbf{G} for each different spectrum curve, where $\mathbf{G}=2\pi/a(n,m)$, n and m are integers and $n,m \leq i$. That is, $N_i=(2i+1)^2-1$, because we must exclude the case of $\mathbf{G}=0$. So, $N_i=8, 24, 48, 80, 120$, and 168 , for $i=1$ up to 6. The spectrum line of the intersubband resonance is clearly enhanced and broadened by adding up the contributions associated with different \mathbf{G} 's. We find that the resonance peaks all occur at $\omega=1.01\omega_{10}$ due to the depolarization shift. The frequencies ω_1 and ω_2 of the maximum and minimum of $dA_p^{(i)}/d\omega$ do not change much, but the difference between the values of the maximum and minimum is enhanced remarkably. As the absorption associated with larger \mathbf{G} is added, outside the ω_1 and ω_2 frequency region, the area under the curve increases. So, the whole absorption derivative spectrum due to dielectric irregularities will be broadened and enhanced by including all possible \mathbf{G} 's.

We also calculate the absorption coefficients for $a=1490, 1980$, and 5950 \AA by including 168 reciprocal vectors \mathbf{G} , up to $i=6$. The shape of the absorption spectrum for these cases appears the same as that for $a=2980 \text{ \AA}$, except that the total absorptions for $a=1980, 2980$, and 5950 \AA are, respectively, about 800, 2.5×10^3 , and 1.3×10^4 times smaller than that for $a=1980 \text{ \AA}$. Since the coupling coefficients $|N(\mathbf{q})|^2$ for larger q 's decay too fast to contribute to absorption coefficients in these three cases, we conclude that there exists some density of the square lattice points that will give the largest resonance peak. The broadening effect at this density will be most effective.

V. CONCLUSION

In this paper, the only assumption we have used is $q \gg (\epsilon_s)^{1/2}\omega/c$. This is the process of indirect photoab-

sorption for the two-dimensional intersubband system. No matter what the polarization of the incident light is, $S(\mathbf{q}, \omega)$, the spectrum function, is all the same to a two-dimensional momentum change $\hbar\mathbf{k} \rightarrow \hbar\mathbf{k} + \hbar\mathbf{q}$ of all possible intersubband transitions $l \rightarrow l'$ ($l, l' = 0, 1, 2, 3, \dots$). The large momentum change $\hbar\mathbf{q}$ parallel to the interface is provided by the impurity particles inside the insulator region. With Eq. (2.15), we can calculate $S(\mathbf{q}, \omega)$ for any mode \mathbf{q} and with Eq. (3.1) sum over all possible \mathbf{q} with the coupling coefficient $|N(\mathbf{q})|^2$, which can be calculated for any model of impurity-particle distribution. With the model we propose in this paper $|N(\mathbf{q})|^2$ is proportional to e^{-2qd} , where d is the distance between the lattice plane and the interface. If d is larger, the coupling coefficients will decay exponentially. So the effective depth for

the impurity particles to enhance absorption is $\sim 1/2q$. Therefore, the surface impurity particles are the dominating source. The bulk impurities buried deeply inside the insulator region give negligible effects to the enhanced absorption.

ACKNOWLEDGMENTS

We are very grateful to Dr. T. W. Nee for introducing this subject and suggesting this investigation. We would like to thank him for providing the copies of his papers prior to publication. Thanks are also extended to S. F. Tasi for her very helpful discussions and for providing us with her M.S. thesis. We want again to thank the National Science Council of the Republic of China for the financial support.

*Present address: Department of Physics, University of California, San Diego, La Jolla, CA 92093.

¹A. Kamgar, P. Kneschaurek, G. Dorda, and F. Koch, Phys. Rev. Lett. **32**, 1251 (1974).

²J. Scholz and F. Koch, Solid State Commun. **34**, 249 (1980).

³H. Reisinger and F. Koch, Solid State Commun. **37**, 429 (1981).

⁴W. Beinvoogl and F. Koch, Solid State Commun. **24**, 687 (1977).

⁵K. Wiesinger, H. Reisinger, and F. Koch, Surf. Sci. **113**, 102 (1982).

⁶T. W. Nee, Phys. Rev. B **29**, 3225 (1984).

⁷T. W. Nee and F. Koch, Phys. Rev. B **29**, 3239 (1984).

⁸F. Stern and W. E. Howard, Phys. Rev. **163**, 816 (1967).

⁹T. Ando, Phys. Rev. B **13**, 3468 (1967).

¹⁰T. Ando, Z. Phys. B **26**, 263 (1977).

¹¹T. Ando, A. Fowler, and F. Stern, Rev. Mod. Phys. **54**, 466 (1982).

¹²Abromowitz and Stegun, *Handbook of Mathematical Functions*, National Bureau of Standards Applied Mathematics Series (U.S. GPO, Washington, D.C., 1964), Chap. 10.

¹³E. Bathe, D. Heitmann, and E. G. Mohr, Physica **117B&118B**, 643 (1983).

¹⁴S. F. Tsai, M.S. thesis, Department of Physics, National Tsing Hua University, Taiwan, 1983 (unpublished).